Hydrol. Earth Syst. Sci. Discuss., 9, 1–22, 2012
www.hydrol-earth-syst-sci-discuss.net/9/1/2012/
doi:10.5194/hessd-9-1-2012

Hydrology and Earth System Sciences Discussions

A framework for upscaling short-term process-level understanding to longer time scales

W. H. Lim[1,3] **and M. L. Roderick**[1,2,3]

[1]Research School of Biology, The Australian National University, Canberra, ACT 0200, Australia
[2]Research School of Earth Sciences, The Australian National University, Canberra, ACT 0200, Australia
[3]Australian Research Council Centre of Excellence for Climate System Science, Australia

Received: 2 May 2012 – Accepted: 2 May 2012 – Published:

Correspondence to: M. L. Roderick (michael.roderick@anu.edu.au)

Published by Copernicus Publications on behalf of the European Geosciences Union.

Abstract

General experience in hydrologic modelling suggests that the parameterisation of a model could change over different time scales. As a result, hydrologists often re-parameterise their models whenever different temporal resolutions are required. Here, we investigate theoretical aspects of this issue in a search for the cause(s) of the need for re-parameterisations. Based on Taylor series expansion, we present a mathematical framework for temporal upscaling and evaluate it using a simple experimental system. For that, we use a unique database of half-hourly pan evaporation measurements (comprising 237 days) and examine how the model parameters change for daily and monthly integration periods. We show that the model parameters change over different integration periods with changes in the covariance between the model variables. The theory presented here is general and can be used as a basis for temporal upscaling.

1 Introduction

Thirty years ago, hydrologists had a reasonable empirical knowledge of the typical rates of many basic processes like rainfall, evaporation, infiltration, etc. One of the central challenges at that time was to use that knowledge to say something useful at the larger temporal and spatial scales of typical hydrological interest, e.g., annual runoff from an entire catchment or river basin, flood peak estimation, etc. Thirty years on, the term “scaling-up” invokes images of bores to monitor groundwater levels, flux towers, weirs, satellite images to document the spatial variations, that are all tied together in a spatial database. These tools have proved immensely useful in the scaling of site-specific measurements. However, at the same time, much less attention has been given to the theoretical side of the scaling-up problem (Blöschl and Sivapalan, 1995; McDonnell et al., 2007).

The theoretical side of the problem is dominated by a key task – the need to correctly calculate the space-time averages (Milly and Eagleson, 1987; Rastetter et al., 1992; Hu and Islam, 1997a,b, 1998; Roderick, 1999; Hansen and Jones, 2000; Vogel and Sankarasubramanian, 2003; Rodriguez-Iturbe et al., 2006). That problem is not unique to hydrology – many other environmental disciplines are also grappling with the same basic problem. For example, climate scientists use the term, "sub-grid variability", to summarise two key concepts involving the calculation of space-time averages. The first key concept relates to the representation of various intensive state variables (e.g., pressure, temperature, specific humidity, etc.) in climate models that typically have very large grid cells, and it is known a priori, that the intensive state variables vary spatially within a grid cell. The second issue is how to calculate the fluxes, and thereby the changes over time, when many of the underlying processes are known to be non-linear. This latter issue is of fundamental importance, because ignoring the non-linearity results in biased predictions (Larson et al., 2001). To use the classical example: the natural logarithm of the average of a group of numbers does not equal the average of the natural logarithms of the same group of numbers (Welsh et al., 1988). The difference between those two estimates is the so-called "bias".

Different approaches to handling this bias can be envisaged. The traditional approach is to use larger computers, smaller grid cells and shorter integration periods (e.g., minutes instead of hours, or hours instead of days, etc.). This is a brute-force approach, but at best, it can only reduce the bias, because to account for it completely using a numerical approach would require both infinitesimally small grid cells and time periods which is not possible due to practical computing constraints. An alternative approach is to account for the "bias" by directly estimating it, but to do that requires a clear theoretical understanding of what the "bias" actually is. For example, hydrologic modellers are well-aware that model parameters can change with the temporal resolution of rainfall-runoff models (e.g., Littlewood and Croke, 2008; Wang et al., 2009; Kavetski et al., 2011) but it is difficult to clarify theoretical aspects of the "bias" using a system as complex as a catchment system. Hence, there is a clear advantage in using a simpler system to gain insight into the issue whilst retaining practical hydrologic relevance.

HESSD
9, 1–22, 2012

In this paper we use a unique half-hourly database of high quality pan evaporation measurements (Lim et al., 2012) to examine bias in the model predictions as a function of the model integration period. To do that we examine how the parameters of the vapour transfer function change when integrating from half-hourly to daily or monthly time periods.

2 Statement of the problem

Dalton's equation for evaporation from a wet surface is,

$$E \propto (e_\mathrm{s}(T_\mathrm{s}) - e_\mathrm{a}(T_\mathrm{a})) \tag{1}$$

where E ($\mathrm{m\,s^{-1}}$) is the evaporation rate of liquid water in traditional hydrologic units of depth per unit time, $e_\mathrm{s}(T_\mathrm{s})$ (Pa) is the vapour pressure at the evaporating surface, $e_\mathrm{a}(T_\mathrm{a})$ (Pa) is the air vapour pressure at the same height that air temperature is measured at.

The scaling of Eq. (1) over a given period (0 to τ) can be written as

$$\frac{1}{\tau}\int_0^\tau E\,\mathrm{d}t \propto \frac{1}{\tau}\int_0^\tau (e_\mathrm{s}(T_\mathrm{s}) - e_\mathrm{a}(T_\mathrm{a}))\,\mathrm{d}t$$

$$\overline{E(\tau)} = f_v(\tau)\overline{(e_\mathrm{s}(T_\mathrm{s}) - e_\mathrm{a}(T_\mathrm{a}))} \tag{2}$$

where $f_v(\tau)$ ($\mathrm{m\,s^{-1}\,Pa^{-1}}$) is the so-called aerodynamic function. The numerical value of $f_v(\tau)$ generally depends on the integration period τ. In that sense, $f_v(\tau)$ can be called an effective parameter (McNaughton, 1994). It is effective in the sense that it will give the correct estimate of $\overline{E(\tau)}$ because it is calculated from observations using $\overline{E(\tau)}/\overline{(e_\mathrm{s}(T_\mathrm{s}) - e_\mathrm{a}(T_\mathrm{a}))}$. That procedure means that if the time period of the model was changed $f_v(\tau)$ might change.

HESSD
9, 1–22, 2012

The correct scaling procedure is to begin with the full equation,

$$
\begin{aligned}
E &= f_v(e_\mathrm{s}(T_\mathrm{s}) - e_\mathrm{a}(T_\mathrm{a})) \\
\frac{1}{\tau}\int_0^\tau E \,\mathrm{d}t &= \frac{1}{\tau}\int_0^\tau f_v(e_\mathrm{s}(T_\mathrm{s}) - e_\mathrm{a}(T_\mathrm{a}))\,\mathrm{d}t \\
\overline{E} &= \overline{f_v(e_\mathrm{s}(T_\mathrm{s}) - e_\mathrm{a}(T_\mathrm{a}))}
\end{aligned}
\tag{3}
$$

where f_v ($\mathrm{m\,s^{-1}\,Pa^{-1}}$) is the aerodynamic function that is independent of the integration period. By inspection we see that the correct procedure is to calculate the mean of the product (Eq. 3) and not the product of the means (Eq. 2). To investigate the differences between Eqs. (2) and (3), we examine the scaling from short-term (e.g., half-hourly) to long-term integration periods (e.g., daily, monthly).

3 Theory

Based on Taylor series expansion, the theory of integrating the product of two variables (e.g., $z = ab$) over a given time period (0 to τ) can be expressed as (see Appendix A for formal derivation)

$$
\begin{aligned}
z &= ab \\
\frac{1}{\tau}\int_0^\tau z \,\mathrm{d}t &= \frac{1}{\tau}\int_0^\tau ab \,\mathrm{d}t \\
\overline{z} &= \overline{ab} \\
&= \overline{a}\;\overline{b} + \sigma_{ab} \\
&= \overline{a}\;\overline{b} + r_{[a,b]}\sigma_a\sigma_b
\end{aligned}
\tag{4}
$$

HESSD
9, 1–22, 2012

W. H. Lim and
M. L. Roderick

where σ_{ab} is the covariance between a and b, $r_{[a,b]}$ (range: −1.0 to 1.0) is the correlation between a and b, σ_a is the population standard deviation of a and σ_b is the population standard deviation of b. Note that this result is independent of the distribution of the variables. If $r_{[a,b]} \to 0$ then $\sigma_{ab} \to 0$ and therefore $\overline{ab} \to \overline{a}\,\overline{b}$. In other words, when the variables are uncorrelated, the mean of the product is equal to the product of the means.

In the more general circumstance, the variables are correlated. We can simplify Eq. (4) by incorporating the coefficient of variation for both a and b (i.e., $C_a \equiv \frac{\sigma_a}{\overline{a}}$ and $C_b \equiv \frac{\sigma_b}{\overline{b}}$),

$$\begin{aligned}\overline{z} &= \overline{a}\,\overline{b}\,(1 + r_{[a,b]}C_aC_b)\\ &= \overline{a}\,\overline{b}\,(1 + \chi_{[a,b]})\end{aligned} \tag{5}$$

where $\chi_{[a,b]}$ is a correction factor arising from the covariance between a and b. Application of Eq. (5) for a product involving more than two variables is demonstrated in Sect. 4.

4 Model system

Following our previous study (Lim et al., 2012), we formulate pan evaporation E_{pan} ($\mathrm{m\,s^{-1}}$) as

$$\begin{aligned}E_{pan} &= f_v(e_s(T_s) - e_a(T_a))\\ &= \frac{M_w}{R\rho_w}\frac{D_v}{T_a}\frac{(e_s(T_s) - e_a(T_a))}{\Delta z}\end{aligned} \tag{6}$$

where f_v ($\mathrm{m\,s^{-1}\,Pa^{-1}}$) is the aerodynamic function, M_w ($\mathrm{kg\,mol^{-1}}$) is the molecular mass of water, R ($\mathrm{J\,mol^{-1}\,K^{-1}}$) is the ideal gas constant, ρ_w ($\mathrm{kg\,m^{-3}}$) is the density of liquid

HESSD
9, 1–22, 2012

water, D_v ($m^2\,s^{-1}$) is the diffusion coefficient for water vapour in air, T_a (K) is the air temperature, Δz is the boundary layer thickness. In our original research, Eq. (6) was parameterised using half-hourly data. Accordingly, we assume the resulting parameters to be effectively instantaneous (these parameters have been tested and found applicable up to 6-hourly integration periods).

Following Eq. (3), scaling of Eq. (6) over longer term periods with constants (M_w, R) and near-constant (ρ_w) removed outside the integration, we have,

$$\overline{E_{pan}} = \frac{M_w}{R\rho_w}\overline{\left[\frac{D_v}{T_a}\frac{(e_s(T_s) - e_a(T_a))}{\Delta z}\right]} \tag{7}$$

Following Eq. (5), we rearrange Eq. (7) as a product of the means, $E^*_{pan} \equiv \frac{M_w}{R\rho_w}\overline{D_v}\,\overline{\frac{1}{T_a}}\,\overline{\frac{1}{\Delta z}}\,(\overline{e_s(T_s)} - \overline{e_a(T_a)})$ that is multiplied by a collection of additive terms that are associated with covariance-based correction factors. In general, for a product involving five variables, there will be ten covariance-based correction factors. In this instance, there is one less because $e_s(T_s)$ and $e_a(T_a)$ are related by a sum (and the mean of a sum equals the sum of the means) and not a product. Using these nine covariance-based correction factors, we have,

$$\begin{aligned}\overline{E_{pan}} \simeq E^*_{pan}\Bigg[1 &+ \chi_{\left[D_v,\frac{1}{T_a}\right]} + \chi_{\left[D_v,\frac{1}{\Delta z}\right]} + \chi_{\left[\frac{1}{T_a},\frac{1}{\Delta z}\right]} + \chi_{[D_v,e_s(T_s)]}\frac{\overline{e_s(T_s)}}{\overline{e_s(T_s)}-\overline{e_a(T_a)}} + \chi_{[D_v,e_a(T_a)]}\left[\frac{-\overline{e_a(T_a)}}{\overline{e_s(T_s)}-\overline{e_a(T_a)}}\right]\\ &+ \chi_{\left[\frac{1}{T_a},e_s(T_s)\right]}\frac{\overline{e_s(T_s)}}{\overline{e_s(T_s)}-\overline{e_a(T_a)}} + \chi_{\left[\frac{1}{T_a},e_a(T_a)\right]}\left[\frac{-\overline{e_a(T_a)}}{\overline{e_s(T_s)}-\overline{e_a(T_a)}}\right]\\ &+ \chi_{\left[\frac{1}{\Delta z},e_s(T_s)\right]}\frac{\overline{e_s(T_s)}}{\overline{e_s(T_s)}-\overline{e_a(T_a)}} + \chi_{\left[\frac{1}{\Delta z},e_a(T_a)\right]}\left[\frac{-\overline{e_a(T_a)}}{\overline{e_s(T_s)}-\overline{e_a(T_a)}}\right]\Bigg]\end{aligned} \tag{8}$$

This is the general equation for temporal upscaling to be examined in later sections.

HESSD
9, 1–22, 2012

5 Data

We use high quality (half-hourly) data collected over 237 days (during 2007–2010) at Canberra, Australia (see details in Lim et al., 2012) for evaluating the magnitude of the covariance-based corrections per Eq. (8). The daily data are aggregated into months (minimum of 16 days to be considered valid). The resulting 11 months included all seasons (2 months in spring, 3 months in summer, 3 months in autumn and 3 months in winter).

6 Evaluating the scaling corrections

6.1 Scaling from instantaneous to daily

The magnitude of the nine covariance-based correction factors (per Eq. 8) when scaling from half-hourly to a daily basis are shown in Fig. 1. We found that most (seven out of nine) of the covariance-based correction factors (i.e., χ) to be approximately zero (Fig. 1a–g). The main reason for the near zero covariance-based correction factors in seven instances is that the coefficient of variation of two variables (D_v and $\frac{1}{T_a}$) is close to zero (results not shown). In contrast, the covariance-based correction factors for the remaining two terms involving the inverse of the boundary layer thickness ($\frac{1}{\Delta z}$) and the two vapour pressures ($e_s(T_s)$, $e_a(T_a)$) were relatively large (Fig. 1h, i). Physically, that makes intuitive sense because we observed a strong diurnal variation where the wind speed tended to increase each afternoon thereby increasing $\frac{1}{\Delta z}$ (Lim et al., 2012) and resulting in a correlation between these variables.

To evaluate the contribution of each covariance-based correction terms to the overall evaporation rate from the pan we plot the partial results (Fig. 2). The results confirmed an underestimate of around 20 % for the daily integrated evaporation rate when the correction terms are ignored (Fig. 2a). Only those corrections involving the inverse of the boundary layer thickness ($\frac{1}{\Delta z}$) and the two vapour pressures ($e_s(T_s)$, $e_a(T_a)$)

made any significant difference to the integration (Fig. 2i, j). With those correction terms the final results showed excellent agreement with observations (Fig. 2k, $R^2 = 0.97$, $n = 237$, RMSE $= 0.50\,\mathrm{mm\,d^{-1}}$).

6.2 Scaling from instantaneous to monthly

We repeated the above analysis but this time we integrated from half-hourly to a monthly period. The results were virtually identical with the earlier analysis based on integration to a daily time period (Fig. 3). Again, only those covariance-based correction factors involving the inverse of the boundary layer thickness ($\frac{1}{\Delta z}$) with the two vapour pressures ($e_s(T_s)$, $e_a(T_a)$) were of practical importance (Fig. 3h, i). If all the covariance-based correction terms were ignored, the bias would result in an underestimate of monthly pan evaporation of around 17 % (Fig. 4a). Including these correction terms gave excellent agreement with the intergated observations (Fig. 4k, $R^2 = 0.99$, $n = 11$, RMSE $= 0.32\,\mathrm{mm\,d^{-1}}$).

6.3 Comparing half-hourly, daily and monthly aerodynamic functions

The previous results have demonstrated that in our application, most of the covariance-based correction factors make little practical difference. Retaining the two important correction factors χ that relate the inverse of the boundary layer thickness ($\frac{1}{\Delta z}$) (which increases with the wind speed) with the two vapour pressures ($e_s(T_s)$, $e_a(T_a)$), we can rewrite Eq. (8) as

$$\overline{E_{\mathrm{pan}}} \approx E^*_{\mathrm{pan}} \left[1 + \chi_{\left[\frac{1}{\Delta z}, e_s(T_s)\right]} \frac{\overline{e_s(T_s)}}{\overline{e_s(T_s)} - \overline{e_a(T_a)}} + \chi_{\left[\frac{1}{\Delta z}, e_a(T_a)\right]} \left[\frac{-\overline{e_a(T_a)}}{\overline{e_s(T_s)} - \overline{e_a(T_a)}} \right] \right] \tag{9}$$

This approximation allows us to express the aerodynamic function $f_v(\tau)$ for long-term pan evaporation measurements from Eq. (2) in terms of the product of the means, denoted f_v^* and the same covariance-based correction factors, we have,

$$f_v(\tau) \approx f_v^* \left[1 + \chi_{\left[\frac{1}{\Delta z}, e_s(T_s)\right]} \frac{\overline{e_s(T_s)}}{\overline{\overline{e_s(T_s)} - \overline{e_a(T_a)}}} + \chi_{\left[\frac{1}{\Delta z}, e_a(T_a)\right]} \left[\frac{-\overline{e_a(T_a)}}{\overline{\overline{e_s(T_s)} - \overline{e_a(T_a)}}} \right] \right] \tag{10}$$

where $f_v^* \equiv \frac{M_w}{R\rho_w} \overline{D_v} \, \overline{\frac{1}{T_a}} \, \overline{\frac{1}{\Delta z}}$. We use that expression to calculate the numerical values of f_v^* at daily ($n = 237$) and monthly ($n = 11$) integration periods and compare those with the original half-hourly results reported by Lim et al. (2012). As anticipated, the long-term (daily, monthly) aerodynamic functions are generally (but not always) numerically larger than the half-hourly values because of the previously noted correlations between $(\frac{1}{\Delta z})$ with $e_s(T_s)$ and $e_a(T_a)$ (Fig. 5).

6.4 Further insights

If short-term data were available it would be straightfoward to numerically estimate the two key covariance-based correction factors (i.e., $\chi_{[\frac{1}{\Delta z}, e_s(T_s)]}$, $\chi_{[\frac{1}{\Delta z}, e_a(T_a)]}$). Without doing that, one could ask whether these correction factors are themselves correlated? If so, one could make further simplifications and possibly avoid the need for detailed calculations. We found that there was no relationship between them at either daily or monthly integration periods (Fig. 6). An alternative approach is to seek a physically justified relationship between these correction factors and a key environmental variable. By defining a new variable, $h^* \equiv \frac{\overline{e_a(T_a)}}{\overline{e_s(T_s)}}$ we can rewrite Eq. (9) as,

$$\overline{E_{pan}} = E_{pan}^* \left[1 + \frac{\chi_{\left[\frac{1}{\Delta z}, e_s(T_s)\right]} - h^* \chi_{\left[\frac{1}{\Delta z}, e_a(T_a)\right]}}{1 - h^*} \right] \tag{11}$$

and Eq. (10) as

$$f_v(\tau) = f_v^* \left[1 + \frac{\chi_{\left[\frac{1}{\Delta z}, e_s(T_s)\right]} - h^* \chi_{\left[\frac{1}{\Delta z}, e_a(T_a)\right]}}{1 - h^*} \right] \tag{12}$$

HESSD
9, 1–22, 2012

W. H. Lim and
M. L. Roderick

We note that $e_s(T_s)$ is not normally observed in standard operational practice. Accordingly, we compare the resulting scaling correction $\frac{\chi_{\left[\frac{1}{\Delta z}, e_s(T_s)\right]} - h^* \chi_{\left[\frac{1}{\Delta z}, e_a(T_a)\right]}}{1-h^*}$ with the observed relative humidity $h \left(\equiv \frac{\overline{e_a(T_a)}}{\overline{e_s(T_a)}} \right)$ over both daily and monthy integration periods (Fig. 7). Over daily integration periods, the resulting scaling corrections varied from $-10\,\%$ to $40\,\%$ with a mean of $\sim 13\,\%$. Over monthly integration periods, the resulting scaling corrections vary from 0 to 20 % with a mean of $\sim 11\,\%$. The overall (but weak) relation to emerge is that the resulting scaling correction approaches zero when the relative humidity approaches saturation (100 %). At the other extreme, when the relative humidity approaches 30 %, the resulting scaling correction approaches 25 %.

In summary, the magnitude of the scaling correction relative to the product of the means (i.e., E^*_{pan}, f^*_v) remain substantial and there does not appear to be a simple way of accurately estimating that as a function of a readily measured environmental variable (e.g., relative humidity).

7 Discussion and summary

The model system used here, i.e., a half-hourly database of high quality pan evaporation measurements, is simpler than the problems typically faced in hydrology, e.g., catchment-scale water balances, etc. By using a simple system we were able to deduce deeper level insights about temporal scaling. In particular, assume an instantaneous physical relationship is accurately known as was the case here for pan evaporation. We showed that the model parameters change for different integration periods because the covariance between model variables changed over those periods. Exact mathematical expressions, based on a Taylor series expansion were developed and used to quantify how the change in covariance propagates into a change in the numerical value of model parameters.

HESSD
9, 1–22, 2012

W. H. Lim and
M. L. Roderick

We followed the above-noted approach using our pan evaporation database and showed that not all covariance-based correction terms actually matter. In our example, there were nine covariance-based correction terms, yet only two of those made any numerical difference to the results. The key physical factor in both was the inverse of the boundary layer thickness ($\frac{1}{\Delta z}$) (which increases with the wind speed). The two important covariance-based correction terms arose from the covariance between (i) $\frac{1}{\Delta z}$ and the vapour pressure at the evaporating surface $e_s(T_s)$ and (ii) $\frac{1}{\Delta z}$ and the air vapour pressure $e_a(T_a)$. With those two correction terms we showed that at this site, the numerical value of the aerodynamic function was generally (but not always) larger at both daily and monthly integration periods compared to the original half-hourly data (Fig. 5). That arose because of a strong diurnal cycle in the pan evaporation data where the wind speed usually peaks in the mid-afternoon each day (Lim et al., 2012).

We found that the resulting scaling correction in the pan evaporation application could be readily understood as a function of the relative humidity (Fig. 7). However, that relation was not sufficiently accurate for routine practical applications. In that sense, the only alternative is to calculate the covariance-based correction using data and theory.

More generally, if we were to handle the question of (temporal) scaling rigorously then we would need to begin reporting the covariances. For example, one regularly sees climatic summaries of averages yet the covariance(s) (or the variance(s) for that matter) are rarely reported. Historically, the use of manual instruments made the reporting of covariances impractical (and more or less impossible). However, with the modern digital instrumentation that is now in routine use it is straightforward to calculate and report covariances. The key challenge is to identify and report the covariances that matter.

Appendix A

Taylor series expansion for a product of two variables

Let $z_i = a_i b_i$ (for $i = 1 \ldots n$) be a product of two variables. We now examine the mean $\bar{z} = \overline{ab}$ by applying a Taylor series expansion in two variables (see any calculus text, e.g., Adams, 1991) about the point $(\bar{a}, \bar{b})$ to express $\bar{z}$ in terms of $\bar{a}$ and $\bar{b}$:

$$\begin{aligned}
\bar{z} &= \frac{1}{n}\sum_{i=1}^{n} z_i \\
&= \frac{1}{n}\sum_{i=1}^{n} z(\bar{a},\bar{b}) + \frac{1}{n}\sum_{i=1}^{n}\left[(a_i-\bar{a})\frac{\partial z}{\partial a_i} + (b_i-\bar{b})\frac{\partial z}{\partial b_i}\right] \\
&\quad + \frac{1}{n}\sum_{i=1}^{n}\frac{1}{2}\left[(a_i-\bar{a})^2\frac{\partial^2 z}{\partial a_i^2} + (a_i-\bar{a})(b_i-\bar{b})\frac{\partial^2 z}{\partial a_i \partial b_i} + (b_i-\bar{b})^2\frac{\partial^2 z}{\partial b_i^2}\right] \\
&\quad + \text{higher order derivatives}
\end{aligned} \tag{A1}$$

where all derivatives are evaluated at $(\bar{a},\bar{b})$. Note that, $\frac{\partial z}{\partial a_i}|_{(\bar{a},\bar{b})} = \bar{b}$, $\frac{\partial z}{\partial b_i}|_{(\bar{a},\bar{b})} = \bar{a}$, $\frac{\partial^2 z}{\partial a_i^2}|_{(\bar{a},\bar{b})} = 0$, $\frac{\partial^2 z}{\partial b_i^2}|_{(\bar{a},\bar{b})} = 0$, $\frac{\partial^2 z}{\partial a_i b_i}|_{(\bar{a},\bar{b})} = 1$, and that all higher order derivatives are zero. Further, we also have,

$$\frac{1}{n}\sum_{i=1}^{n}(a_i-\bar{a}) = \frac{1}{n}\sum_{i=1}^{n} a_i - \frac{n\bar{a}}{a} = \bar{a}-\bar{a} = 0 \tag{A2}$$

and similarly,

$$\frac{1}{n}\sum_{i=1}^{n}(b_i-\bar{b}) = 0 \tag{A3}$$

HESSD
9, 1–22, 2012
Scaling theory
W. H. Lim and M. L. Roderick

Thus, Eq. (A1) becomes,

$$\bar{z} = \overline{a\,b} = \bar{a}\,\bar{b} + \frac{1}{2}(0 + 2\sigma_{ab} + 0) = \bar{a}\,\bar{b} + \sigma_{ab} \tag{A4}$$

where σ_{ab} is the covariance between variables a and b. Note that the covariance term emerges from the mathematics of the Taylor series expansion, and thus this result is independent of the underlying distributions of a and b.

Acknowledgements. We thank Belinda Barnes and Stephen Roxburgh who contributed ideas for earlier work on this topic. We acknowledge the Australian Research Council (ARC) for the financial support of this study through the grants DP0879763 and CE11E0098.

References

Adams, R. A.: Calculus: A Complete Course, Addison-Wesley, Reading, MA, 1991. 13

Blöschl, G. and Sivapalan, M.: Scale issues in hydrological modelling: a review, Hydrol. Process., 9, 251–290, doi:10.1002/hyp.3360090305, 1995. 2

Hansen, J. W. and Jones, J. W.: Scaling-up crop models for climate variability applications, Agr. Syst., 65, 43–72, doi:10.1016/S0308-521X(00)00025-1, 2000. 3

Hu, Z. L. and Islam, S.: Effects of spatial variability on the scaling of land surface parameterizations, Bound.-Lay. Meteorol., 83, 441–461, doi:10.1023/A:1000367018581, 1997a. 3

Hu, Z. L. and Islam, S.: A framework for analyzing and designing scale invariant remote sensing algorithms, IEEE T. Geosci. Remote, 35, 747–755, doi:10.1109/36.581996, 1997b. 3

Hu, Z. L. and Islam, S.: Effects of subgrid-scale heterogeneity of soil wetness and temperature on grid-scale evaporation and its parametrization, Int. J. Climatol., 18, 49–63, doi:10.1002/(SICI)1097-0088(199801)18:1<49::AID-JOC224>3.0.CO;2-U, 1998. 3

Kavetski, D., Fenicia, F., and Clark, M. P.: Impact of temporal data resolution on parameter inference and model identification in conceptual hydrological modeling: insights from an experimental catchment, Water Resour. Res., 47, W05501, doi:10.1029/2010WR009525, 2011. 3

Larson, V. E., Wood, R., Field, P. R., Golaz, J. C., Vonder Haar, T. H., and Cotton, W. R.: Systematic biases in the microphysics and thermodynamics of numerical models that ignore subgrid-scale variability, J. Atmos. Sci., 58, 1117–1128, doi:10.1175/1520-0469(2001)058<1117:sbitma>2.0.co;2, 2001. 3

Littlewood, I. G. and Croke, B. F. W.: Data time-step dependency of conceptual rainfall-streamflow model parameters: an empirical study with implications for regionalisation, Hydrol. Sci. J., 53, 685–695, doi:10.1623/hysj.53.4.685, 2008. 3

Lim, W. H., Roderick, M. L., Hobbins, M. T., Wong, S. C., Groeneveld, P. J., Sun, F., and Farquhar, G. D.: The aerodynamics of pan evaporation, Agr. Forest Meteorol., 152, 31–43, doi:10.1016/j.agrformet.2011.08.006, 2012. 4, 6, 8, 10, 12

McDonnell, J. J., Sivapalan, M., Vache, K., Dunn, S., Grant, G., Haggerty, R., Hinz, C., Hooper, R., Kirchner, J., Roderick, M. L., Selker, J., and Weiler, M.: Moving beyond heterogeneity and process complexity: a new vision for watershed hydrology, Water Resour. Res., 43, W07301, doi:10.1029/2006WR005467, 2007. 2

McNaughton, K. G.: Effective stomatal and boundary-layer resistances of heterogeneous surfaces, Plant Cell Environ., 17, 1061–1068, doi:10.1111/j.1365-3040.1994.tb02029.x, 1994. 4

Milly, P. C. D. and Eagleson, P. S.: Effects of spatial variability on annual average water balance, Water Resour. Res., 23, 2135–2143, doi:10.1029/WR023i011p02135, 1987. 2

Rastetter, E. B., King, A. W., Cosby, B. J., Hornberger, G. M., Oneill, R. V., and Hobbie, J. E.: Aggregating fine-scale ecological knowledge to model coarser-scale attributes of ecosystems, Ecol. Appl., 2, 55–70, 1992. 2

Roderick, M. L.: Estimating the diffuse component from daily and monthly measurements of global radiation, Agr. Forest Meteorol., 95, 169–185, doi:10.1016/S0168-1923(99)00028-3, 1999. 3

Rodriguez-Iturbe, I., Isham, V., Cox, D. R., Manfreda, S., and Porporato, A.: Space-time modeling of soil moisture: stochastic rainfall forcing with heterogeneous vegetation, Water Resour. Res., 42, W06D05, doi:10.1029/2005WR004497, 2006. 3

Vogel, R. M. and Sankarasubramanian, A.: Validation of a watershed model without calibration, Water Resour. Res., 39, 1292, doi:10.1029/2002WR001940, 2003. 3

Wang, Y., He, B., and Takase, K.: Effects of temporal resolution on hydrological model parameters and its impact on prediction of river discharge, Hydrol. Sci. J., 54, 886–898, doi:10.1623/hysj.54.5.886, 2009. 3

Welsh, A. H., Peterson, A. T., and Altmann, S. A.: The fallacy of averages, Am. Nat., 132, 277–288, 1988. 3

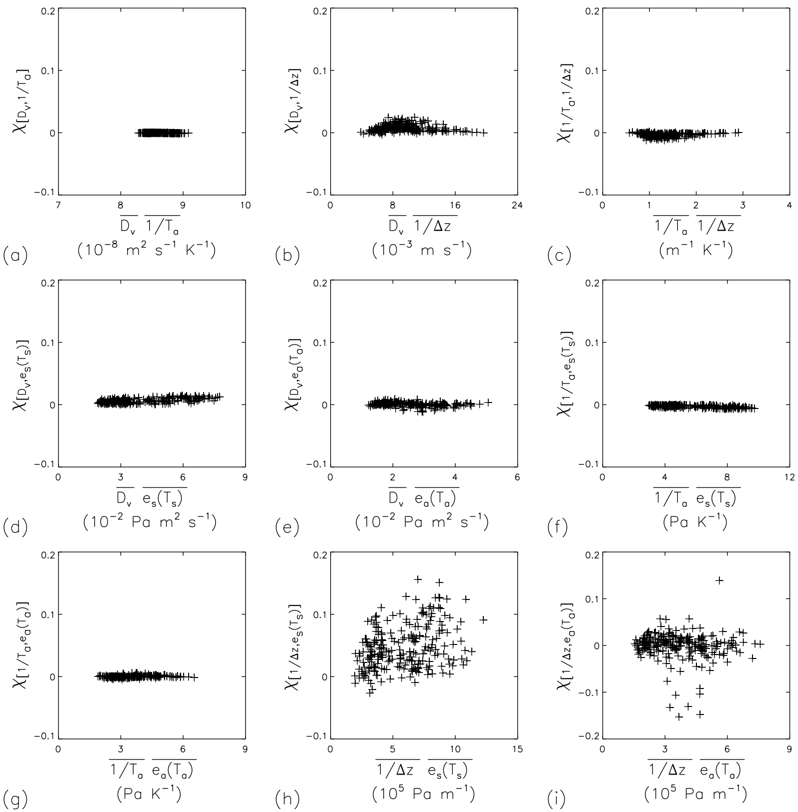

Fig. 1. Relation between the covariance-based correction factors (per Eq. 8) and the relevant product of the means for all nine combination for 237 days as follows: **(a)** D_v, $\frac{1}{T_\mathrm{a}}$, **(b)** D_v, $\frac{1}{\Delta z}$, **(c)** $\frac{1}{T_\mathrm{a}}$, $\frac{1}{\Delta z}$, **(d)** D_v, $e_\mathrm{s}(T_\mathrm{s})$, **(e)** D_v, $e_\mathrm{a}(T_\mathrm{a})$, **(f)** $\frac{1}{T_\mathrm{a}}$, $e_\mathrm{s}(T_\mathrm{s})$, **(g)** $\frac{1}{T_\mathrm{a}}$, $e_\mathrm{a}(T_\mathrm{a})$, **(h)** $\frac{1}{\Delta z}$, $e_\mathrm{s}(T_\mathrm{s})$, **(g)** $\frac{1}{T_\mathrm{a}}$, $e_\mathrm{a}(T_\mathrm{a})$, **(h)** $\frac{1}{\Delta z}$, $e_\mathrm{s}(T_\mathrm{s})$, **(i)** $\frac{1}{\Delta z}$, $e_\mathrm{a}(T_\mathrm{a})$.

HESSD
9, 1–22, 2012

W. H. Lim and
M. L. Roderick

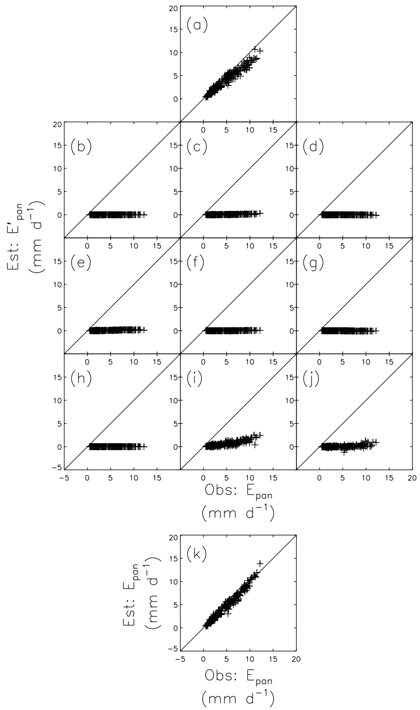

Fig. 2. Estimated E_{pan} (Eq. 8; prime symbol (′) denotes partial results) versus observed E_{pan} for 237 days: **(a)** E^*_{pan}, **(b)** $\chi_{[D_\mathrm{v},\frac{1}{T_\mathrm{a}}]}\,E^*_{\mathrm{pan}}$, **(c)** $\chi_{[D_\mathrm{v},\frac{1}{\Delta z}]}\,E^*_{\mathrm{pan}}$, **(d)** $\chi_{[\frac{1}{T_\mathrm{a}},\frac{1}{\Delta z}]}\,E^*_{\mathrm{pan}}$, **(e)** $\chi_{[D_\mathrm{v},e_\mathrm{s}(T_\mathrm{s})]}\,\frac{\overline{e_\mathrm{s}(T_\mathrm{s})}}{\overline{e_\mathrm{s}(T_\mathrm{s})-e_\mathrm{a}(T_\mathrm{a})}}\,E^*_{\mathrm{pan}}$, **(f)** $\chi_{[D_\mathrm{v},e_\mathrm{a}(T_\mathrm{a})]}\left[\frac{-\overline{e_\mathrm{a}(T_\mathrm{a})}}{\overline{e_\mathrm{s}(T_\mathrm{s})-e_\mathrm{a}(T_\mathrm{a})}}\right]E^*_{\mathrm{pan}}$, **(g)** $\chi_{[\frac{1}{T_\mathrm{a}},e_\mathrm{s}(T_\mathrm{s})]}\,\frac{\overline{e_\mathrm{s}(T_\mathrm{s})}}{\overline{e_\mathrm{s}(T_\mathrm{s})-e_\mathrm{a}(T_\mathrm{a})}}\,E^*_{\mathrm{pan}}$, **(h)** $\chi_{[\frac{1}{T_\mathrm{a}},e_\mathrm{a}(T_\mathrm{a})]}\left[\frac{-\overline{e_\mathrm{a}(T_\mathrm{a})}}{\overline{e_\mathrm{s}(T_\mathrm{s})-e_\mathrm{a}(T_\mathrm{a})}}\right]E^*_{\mathrm{pan}}$, **(i)** $\chi_{[\frac{1}{\Delta z},e_\mathrm{s}(T_\mathrm{s})]}\,\frac{\overline{e_\mathrm{s}(T_\mathrm{s})}}{\overline{e_\mathrm{s}(T_\mathrm{s})-e_\mathrm{a}(T_\mathrm{a})}}\,E^*_{\mathrm{pan}}$, **(j)** $\chi_{[\frac{1}{\Delta z},e_\mathrm{a}(T_\mathrm{a})]}\left[\frac{-\overline{e_\mathrm{a}(T_\mathrm{a})}}{\overline{e_\mathrm{s}(T_\mathrm{s})-e_\mathrm{a}(T_\mathrm{a})}}\right]E^*_{\mathrm{pan}}$, **(k)** sum of **(a)** to **(j)** (Regression: 0.99x – 0.14, $R^2 = 0.97$, $n = 237$, RMSE = 0.50 mm d^{-1}).

HESSD
9, 1–22, 2012

W. H. Lim and
M. L. Roderick

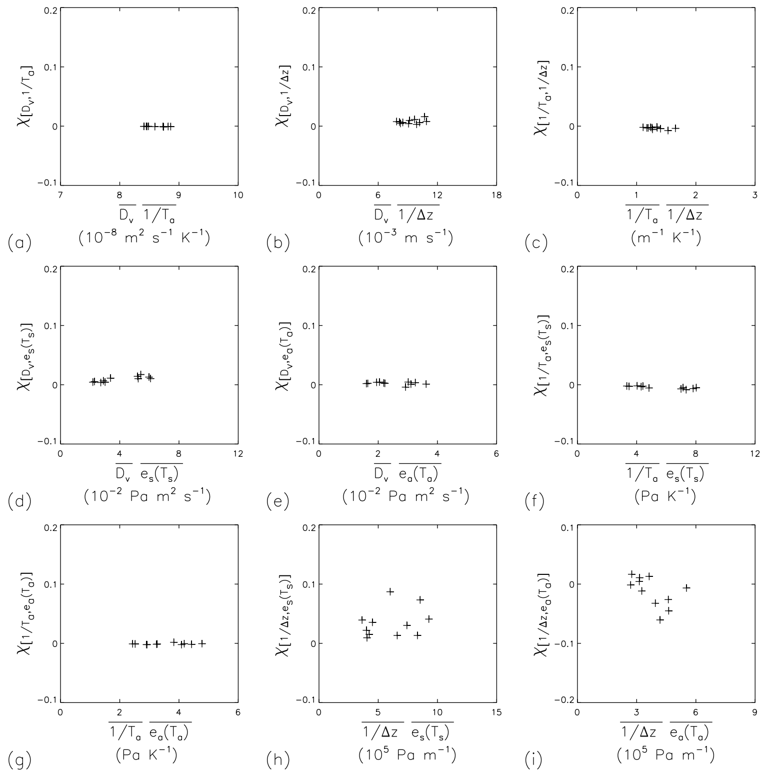

Fig. 3. Relation between the covariance-based correction factors (per Eq. 8) and the relevant product of the means for all nine combination for 11 months as follows: **(a)** D_v, $\frac{1}{T_a}$, **(b)** D_v, $\frac{1}{\Delta z}$, **(c)** $\frac{1}{T_a}$, $\frac{1}{\Delta z}$, **(d)** D_v, $e_s(T_s)$, **(e)** D_v, $e_a(T_a)$, **(f)** $\frac{1}{T_a}$, $e_s(T_s)$, **(g)** $\frac{1}{T_a}$, $e_a(T_a)$, **(h)** $\frac{1}{\Delta z}$, $e_s(T_s)$, **(g)** $\frac{1}{T_a}$, $e_a(T_a)$, **(h)** $\frac{1}{\Delta z}$, $e_s(T_s)$, **(i)** $\frac{1}{\Delta z}$, $e_a(T_a)$.

HESSD
9, 1–22, 2012

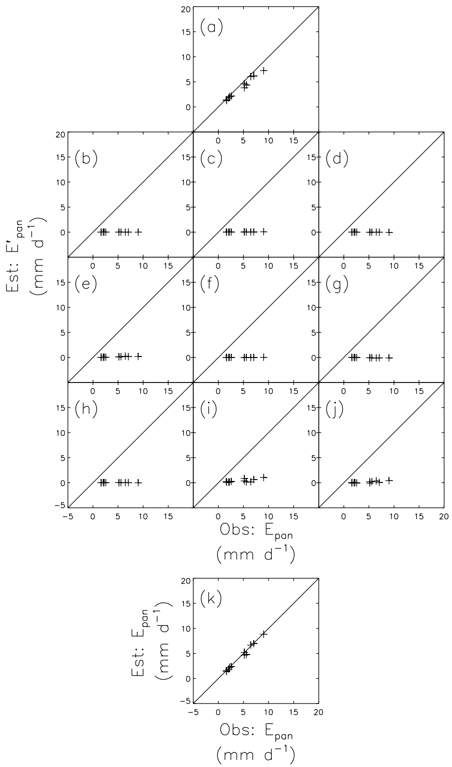

Fig. 4. Estimated E_{pan} (Eq. 8; prime symbol (′) denotes partial results) versus observed E_{pan} for 11 months: **(a)** E^*_{pan}, **(b)** $\chi_{[D_v,\frac{1}{T_a}]}\ E^*_{\text{pan}}$, **(c)** $\chi_{[D_v,\frac{1}{\Delta z}]}\ E^*_{\text{pan}}$, **(d)** $\chi_{[\frac{1}{T_a},\frac{1}{\Delta z}]}\ E^*_{\text{pan}}$, **(e)** $\chi_{[D_v,e_s(T_s)]}\ \dfrac{\overline{e_s(T_s)}}{\overline{e_s(T_s)-e_a(T_a)}}\ E^*_{\text{pan}}$, **(f)** $\chi_{[D_v,e_a(T_a)]}\left[\dfrac{-\overline{e_a(T_a)}}{\overline{e_s(T_s)-e_a(T_a)}}\right] E^*_{\text{pan}}$, **(g)** $\chi_{[\frac{1}{T_a},e_s(T_s)]}\ \dfrac{\overline{e_s(T_s)}}{\overline{e_s(T_s)-e_a(T_a)}}\ E^*_{\text{pan}}$, **(h)** $\chi_{[\frac{1}{T_a},e_a(T_a)]}\left[\dfrac{-\overline{e_a(T_a)}}{\overline{e_s(T_s)-e_a(T_a)}}\right] E^*_{\text{pan}}$, **(i)** $\chi_{[\frac{1}{\Delta z},e_s(T_s)]}\ \dfrac{\overline{e_s(T_s)}}{\overline{e_s(T_s)-e_a(T_a)}}\ E^*_{\text{pan}}$, **(j)** $\chi_{[\frac{1}{\Delta z},e_a(T_a)]}\left[\dfrac{-\overline{e_a(T_a)}}{\overline{e_s(T_s)-e_a(T_a)}}\right] E^*_{\text{pan}}$, **(k)** sum of **(a)** to **(j)** (Regression: 0.99x – 0.15, $R^2 = 0.99$, $n = 11$, RMSE = 0.32 mm d^{-1}).

HESSD
9, 1–22, 2012

Scaling theory

W. H. Lim and
M. L. Roderick

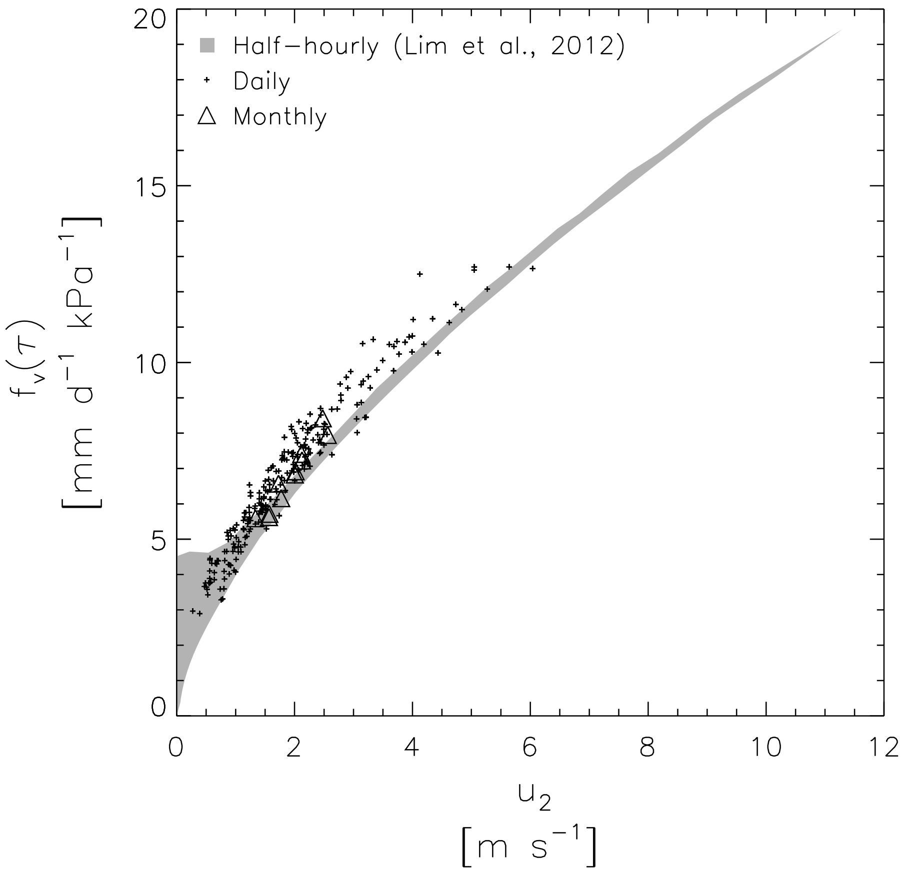

Fig. 5. Estimates of the aerodynamic function $f_v(\tau)$ versus u_2 (wind speed at 2 m above ground level) for the experimental pan for different integration periods.

HESSD
9, 1–22, 2012

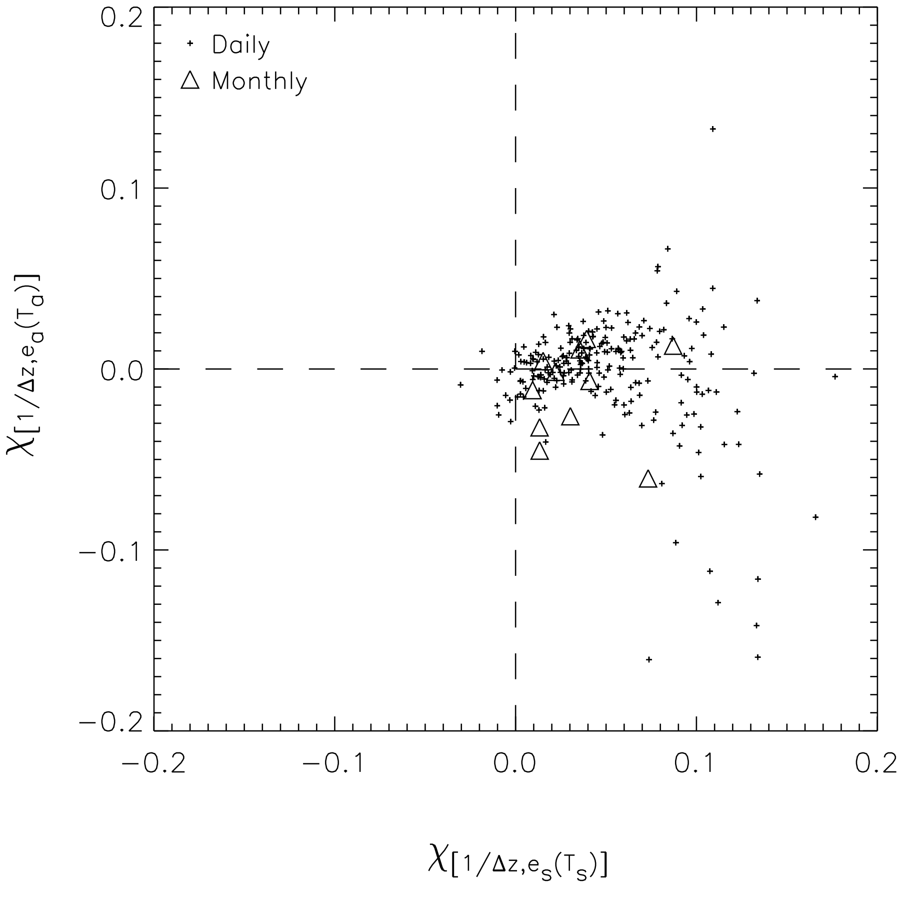

Fig. 6. Relation between the two key covariance-based correction factors for different integration periods.

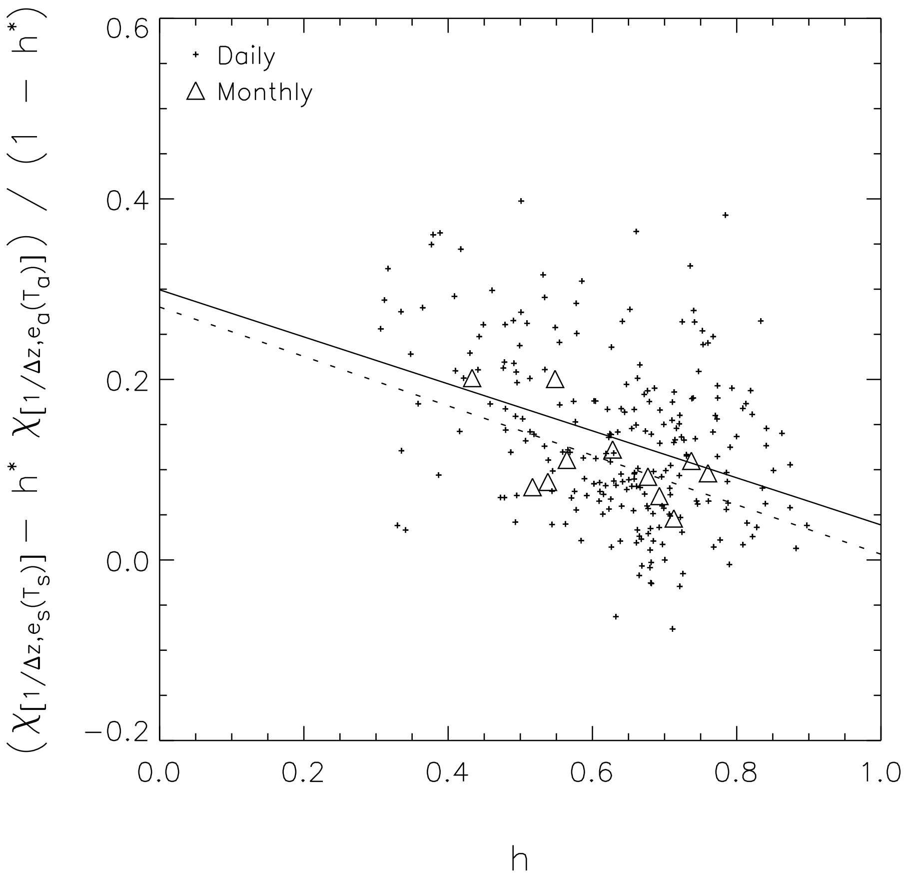

Fig. 7. Relation between the resulting scaling correction (per Eqs. 11 and 12) and the relative humidity for different integration periods (Daily regression (solid line): $-0.26x + 0.30$, $R^2 = 0.13$, $n = 237$; Monthly regression (dotted line): $-0.27x + 0.28$, $R^2 = 0.34$, $n = 11$).

HESSD
9, 1–22, 2012

W. H. Lim and
M. L. Roderick

Title Page
Abstract | Introduction
Conclusions | References
Tables | Figures
◂ | ▸
Back | Close
Full Screen / Esc
Printer-friendly Version
Interactive Discussion